Published for the International Glaciological Society

THIS MANUSCRIPT HAS BEEN SUBMITTED TO THE JOURNAL OF GLACIOLOGY AND HAS NOT BEEN PEER-REVIEWED.

Evidence that seismic anisotropy captures upstream palaeo ice fabric: Implications on present day deformation at Whillans Ice Stream, Antarctica

Journal:	*Journal of Glaciology*
Manuscript ID	JOG-23-0130.R1
Manuscript Type:	Article
Date Submitted by the Author:	n/a
Complete List of Authors:	Leung, Justin; Oxford University, Department of Earth Sciences Hudson, Thomas; Oxford University, Department of Earth Sciences Kendall, John-Michael; Oxford University, Department of Earth Sciences Barcheck, Grace; Cornell University, Department of Earth and Atmospheric Sciences
Keywords:	Ice streams, Seismology, Anisotropic ice
Abstract:	Understanding deformation and slip at ice streams, which are responsible for 90 % of Antarctic ice loss, is vital for accurately modelling large-scale ice flow. Ice preferred crystal orientation fabric (COF) has a first-order effect on ice stream deformation. For the first time, we use shear-wave splitting (SWS) measurements of basal icequakes at Whillans Ice Stream (WIS), Antarctica, to determine a shear-wave anisotropy with an average delay time of 7 ms and fast S-wave polarisation (φ) of 29.3º. The polarisation is expected to align perpendicular to ice flow, whereas our observation is oblique to the current ice flow direction (~280º). Our results suggest that ice at WIS preserves upstream fabric caused by palaeo-deformation developed over at least the past 450 years, implying that changes in the shape of WIS occurs on timescales shorter than COF re-equilibration. The "palaeo-fabric" can somewhat control present-day ice flow, which we suggest may somewhat counteract the long-term slowdown at WIS. Our findings suggest that seismic anisotropy can provide information on past ice

	sheet dynamics, and how past ice dynamics can play a role in controlling current deformation.

Journal of Glaciology, Vol. 70, No. 3, 2023

Evidence that seismic anisotropy captures upstream palaeo ice fabric: Implications on present day deformation at Whillans Ice Stream, Antarctica

Justin LEUNG,[1] Thomas HUDSON,[1] John-Michael KENDALL,[1] Grace BARCHECK[2]

[1]*Department of Earth Sciences, University of Oxford, Oxford, UK*

[2]*Department of Earth and Atmospheric Sciences, Cornell University, Ithaca, NY, USA*

Correspondence: Justin Leung <justin.leung@earth.ox.ac.uk>

ABSTRACT. Understanding deformation and slip at ice streams, which are responsible for 90 % of Antarctic ice loss, is vital for accurately modelling large-scale ice flow. Ice crystal orientation fabric (COF) has a first-order effect on ice stream deformation. For the first time, we use shear-wave splitting (SWS) measurements of basal icequakes at Whillans Ice Stream (WIS), Antarctica, to determine a shear-wave anisotropy with an average delay time of 7 ms and fast S-wave polarisation (φ) of 29.3°. The polarisation is expected to align perpendicular to ice flow, whereas our observation is oblique to the current ice flow direction (~280°). Our results suggest that ice at WIS preserves upstream fabric caused by palaeo-deformation developed over at least the past 450 years, implying that changes in the shape of WIS occurs on timescales shorter than COF re-equilibration. The "palaeo-fabric" can somewhat control present-day ice flow, which we suggest may somewhat counteract the long-term slowdown at WIS. Our findings suggest that seismic anisotropy can provide information on past ice sheet dynamics, and how past ice dynamics can play a role in controlling current deformation.

INTRODUCTION

Despite ice streams spanning only 10 % of Antarctica's surface area, they are responsible for 90 % of Antarctic ice loss (Morgan and others, 1982). Therefore, studying ice stream rheology is important for understanding Antarctica's contribution to sea-level rise. One source of uncertainty in ice stream dynamics is the effect of ice fabrics on rheology, where ice with a crystal oriented fabric (COF) can be ten times weaker in shear in a particular direction relative to isotropic ice (Budd and Jacka, 1989; Pimienta and others, 1987). Glacial ice is formed of anisotropic grains with hexagonal crystalline symmetry, such that the viscosity along the basal plane of ice (normal to c-axis) is sixty times less than that perpendicular to it (Duval and others, 1983). Under stress, the c-axes in a bulk polycrystalline ice mass can rotate to form an ice COF over timescales of hundreds of years, which can change in response to the stress it encounters (Azuma, 1994). Hence, understanding ice COF provides insight on past deformation history and how it might influence future ice flow.

Most glacial ice COF measurements are taken from microstructural analyses of ice core samples. However, these are usually measured from stable or slow-moving regions of ice sheets, and cannot provide much information of the physical processes in fast-deforming regions (Fan and others, 2021; Llorens and others, 2022). In contrast, seismic anisotropy measurements can be used to deduce ice COF properties over large areas in different ice settings, including ice streams (Smith and others, 2017). Therefore, seismic anisotropy can provide insight in these key fast-flowing regions, which can inform models of ice-sheet dynamics.

Whillans Ice Stream (WIS) is a major ice stream in West Antarctica that flows into the Ross Sea embayment (see Figure 1; Picotti and others, 2015). The downstream portion of WIS is known as Whillans Ice Plain (WIP), and it flows at a speed of over 300 metres per year, with stable sliding of the ice stream punctuated 1-2 times daily by sudden unstable sliding motion during 30-minute slip events that also produce high frequency icequakes and tremor (Barcheck and others, 2018; Bindschadler and others, 2003; Winberry and others, 2013). Long-term slowdown of the ice stream can be seen, with longer periods of quiescence between slip events over time, suggesting possibility of future stagnation (Winberry and others, 2014). WIS is an excellent area to study basal seismicity given that seismic and global navigation satellite system data have been collected over recent decades at numerous sites to study its stick-slip cycle (e.g. Barcheck and others, 2020; Pratt and others, 2014; Walter and others, 2011, 2015; Winberry and others, 2009, 2011) and basal hydrologic cycle (e.g. Fricker and Scambos, 2009; Siegfried and others, 2016).

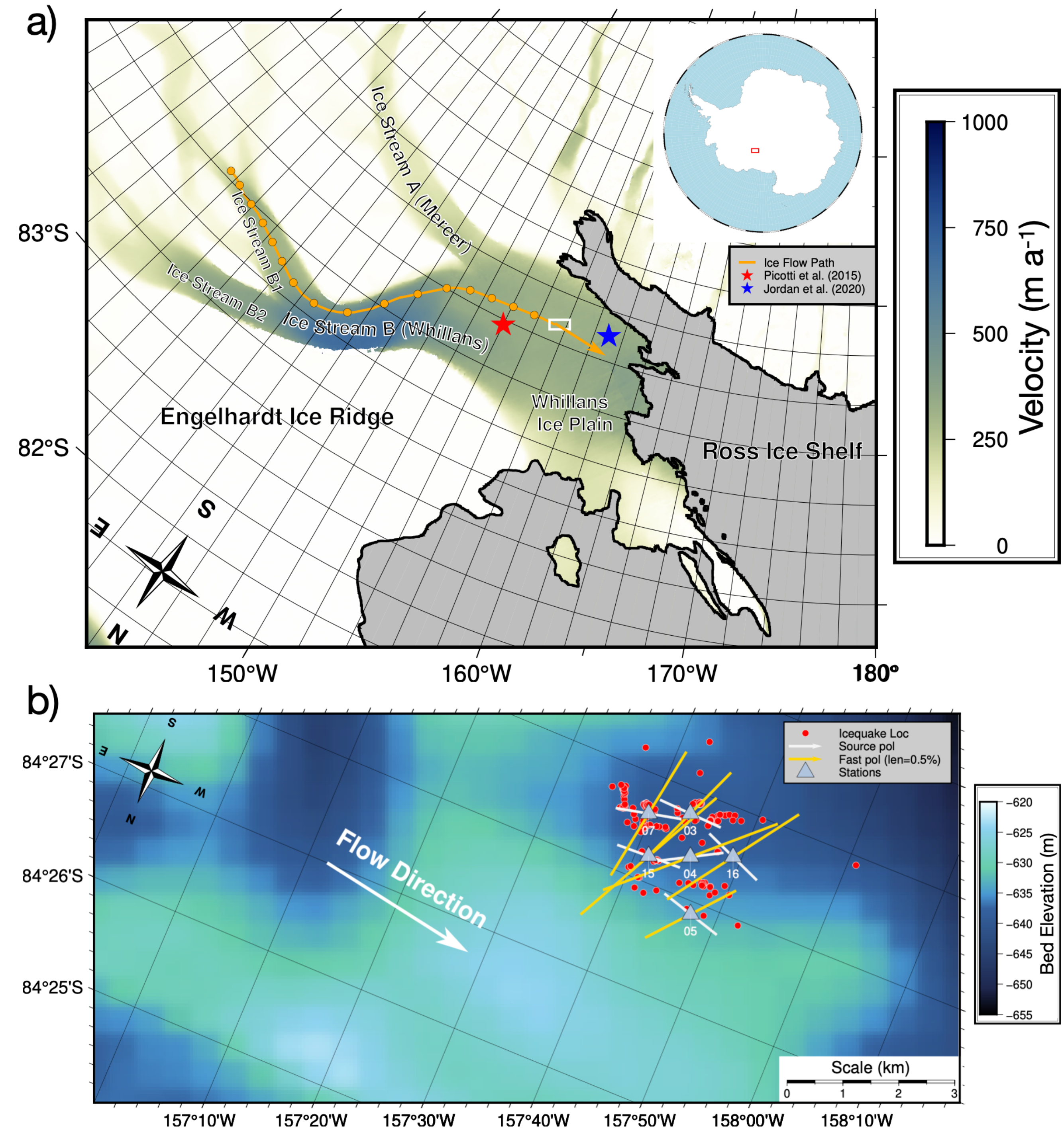
a)
Ice Stream A (Mercer)
Ice Stream B1
Ice Stream B2
Ice Stream B (Whillans)
Engelhardt Ice Ridge
Whillans
Ice Plain
Ross Ice Shelf
Ice Flow Path
Picotti et al. (2015)
Jordan et al. (2020)
83°S
82°S
150°W
160°W
170°W
180°
S
E
W
N
1000
750
500
250
0
Velocity (m a^{-1})
b)
Flow Direction
Icequake Loc
Source pol
Fast pol (len=0.5%)
Stations
07
03
15
04
16
05
84°27'S
84°26'S
84°25'S
157°10'W
157°20'W
157°30'W
157°40'W
157°50'W
158°00'W
158°10'W
Scale (km)
0
1
2
3
−620
−625
−630
−635
−640
−645
−650
−655
Bed Elevation (m)

Fig. 1. Stereographic maps showing Whillans Ice Stream (WIS) and study location. (a) Regional map of the WIS. The grounding line is marked in the thick black line, and the grey shaded areas mark regions of floating ice. The blue and red star show the study site locations of Jordan and others (2020) and Picotti and others (2015) respectively. The orange line outlines the upstream flow path of the ice at our study site location, assuming current flow velocities, with orange points marking the locations at intervals of 50 years (see supplementary information for flow path calculation). The background colour map shows the ice flow velocity obtained from MEaSUREs InSAR-Based Antarctica Ice Velocity Map, Version 2 (Rignot and others, 2017). The study area in (b) is outlined by the white box. (b) Detailed map of the study region. Stations are marked as blue triangles, and icequake locations are shown by red scatter points. Gold lines show the fast S-wave polarisation direction, with the length of the line representing the strength of anisotropy. White lines show the source polarisations for each event, as estimated from recorded shear waves. Dominant ice flow direction (280°) is indicated by the large white arrow. The background colour map shows the bed elevation Morlighem (2022).

There are currently little ice COF observations for the entire ice column at WIS. Picotti and others (2015) used active seismic sources to suggest an azimuth-independent vertically transverse isotropic fabric (VTI) at WIS, with a focus on the top 200 metres. Conversely, Jordan and others (2020) used electromagnetic methods to argue that the c-axes orient parallel to flow at WIS by polarimetric radar sounding that measured the top 400 metres of WIS (see Figure 1 for locations). Here, we provide the first seismic anisotropy measurements from shear-wave splitting of basal icequakes of the entire ice column at Whillans Ice Stream.

METHODOLOGY

This study uses 319 icequakes recorded between January 20th and February 27th, 2014 by six seismometers at Whillans Ice Plain, Antarctica, part of a network active between 2012 to 2018 (Barcheck and others, 2020; Schwartz, 2012). The ice at the study site is between 690 and 710 m thick (Barcheck and others, 2020) and moving at $\sim$370 ma^{-1} (Morlighem, 2022). Since horizontal orientation of the instruments is important for studying seismic anisotropy, we verified the orientation of these instruments using a teleseismic event. We performed a manual search for icequakes focused within the duration of bidaily slip events at WIS, described in Barcheck and others (2021). Icequake arrival times are picked manually and are located using NonLinLoc, a probabilistic non-linear earthquake location algorithm (Lomax and others, 2000). Only icequakes originating at the bed of the ice stream are of interest for measuring total anisotropy in the ice column, therefore icequakes with a source depth shallower than 400 metres are removed. Each icequake is filtered by a 10-100 Hz bandpass filter, based on the dominant source spectra of the icequakes (see Figure S1). Seismic anisotropy is analysed on the horizontal (north and east) components because a ∼100 m thick firn layer refracts the ray path of icequakes to near-vertical incidence at the surface (Picotti and others, 2015).

Shear-wave splitting (SWS) analysis is conducted using the python package SWSPy (Hudson and others, 2023a), based on the approach of Wuestefeld and others (2010). It can be summarised as follows: First, a range of analysis time windows are defined because SWS measurements are sensitive to window lengths (Teanby and others, 2004). Second, a grid search is performed over fast shear-wave polarisation of -90°$< \varphi \leqslant$ 90° and delay times between fast and slow S-waves of $0 \leqslant \delta t \leqslant 0.1$ for each window, such that $\varphi = 0$ represents a fast shear-wave polarisation in the north (and south) direction. The splitting parameters, φ and δt, associated with the minimum second eigenvalue of the S-wave covariance matrix that best linearize particle motion, describe the anisotropy observed along a given source-receiver ray path. Third, density-based cluster analysis is performed on all optimal φ and δt values, such that the optimal φ and δt values are obtained from the most stable cluster with minimum variance in φ and δt (Ester and others, 1996; Teanby and others, 2004). The source polarisation is then calculated by taking the azimuth of the largest eigenvalue of the covariance matrix of the linearised waveforms (Walsh and others, 2013).

A well-constrained result after SWS correction is defined as satisfying the following four requirements: (1) the particle motion (see Figure 2c) becomes approximately linear after removing splitting using the optimal SWS parameters, (2) the error surface (see Figure 2f) has a unique, well-constrained solution, (3) splitting parameters (φ and δt) are stable (see Figure 2e) throughout different clusters, and (4) the quality factor Q_w is larger than 0.7. Q_w measures the robustness of the splitting measurement, and it is calculated by comparing the results from the eigenvalue method of Silver and Chan (1991) to the cross-correlation method of Menke and Levin (2003). A value of $Q_w = 1$ signifies a perfect match between the two methods, $Q_w =$ -1 a good null result, and $Q_w = 0$ a poor result (Wuestefeld and others, 2010).

The strength of anisotropy (δV), or the difference between fast and slow S-wave velocities, can be quantified by the change in velocity, derived from the delay time (δt):

$$\delta V = (V \times \delta t \times 100)/r \tag{1}$$

where $V = 1944$ ms^{-1} is the average isotropic shear-wave speed (Smith and others, 2017) and r the source-receiver distance.

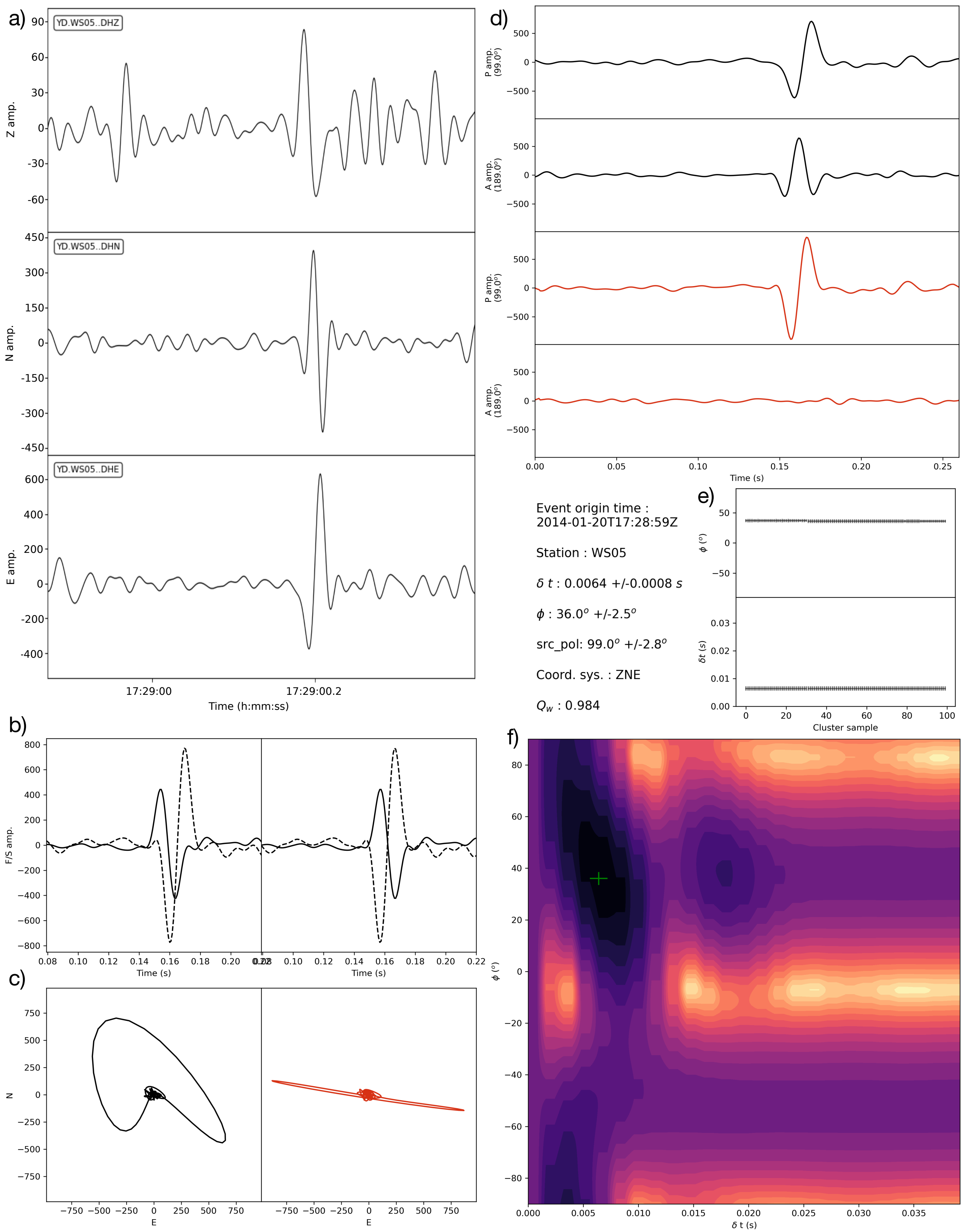
a)
YD.WS05..DHZ
Z amp.
YD.WS05..DHN
N amp.
YD.WS05..DHE
E amp.
17:29:00
17:29:00.2
Time (h:mm:ss)
b)
F/S amp.
Time (s)
c)
N
E
d)
P amp. (99.0°)
A amp. (189.0°)
Time (s)
Event origin time : 2014-01-20T17:28:59Z
Station : WS05
δ t : 0.0064 +/-0.0008 s
φ : 36.0° +/-2.5°
src_pol: 99.0° +/-2.8°
Coord. sys. : ZNE
Q_w : 0.984
e)
φ (°)
δt (s)
Cluster sample
f)
φ (°)
δ t (s)

Fig. 2. An example of a well-constrained shear-wave splitting event. (a) Icequake signal before correction in the vertical, north and east component. (b) The waveforms before (left) and after (right) SWS correction, plotted in the fast (black line) and slow (dotted) directions. (c) Horizontal (north and east) particle motion before (left) and after (right) SWS correction. (d) Particle motion of icequakes in the source polarisation (P) and the perpendicular azimuth (A) before (top two) and after (bottom two) correction. (e) Optimal φ and δt for different cluster sizes. A good splitting measurement should have constant φ and δt values independent of cluster size. (f) Error surface plotted on φ vs δt. Larger errors are represented with brighter colours, and smaller errors with darker colours. The optimal φ and δt and its uncertainties are shown with the green symbol.

RESULTS

80 results from 70 events fulfil the aforementioned four criteria, and therefore are chosen for further analysis. The fast S-wave polarisation φ and source polarisation of these events are plotted as polar histograms in Figure 3. For a double-couple icequake source associated with ice slip at the bed, S-wave source polarisation is aligned with the direction of slip (Hudson and others, 2020). One might typically expect the average S-wave source polarisation to align approximately with ice flow direction. Most source polarisation measurements lie approximately in the east-west direction with an average of 264°N ± 22º (see Figure 3a), which is in agreement with the Whillans Ice Stream's flow direction of 280°N ± 2° (Rignot and others, 2017).

The average delay time for these results is 7.1 ms and ranges from 1.6 ms to 19.2 ms. The average strength of anisotropy, δV, is ∼1.5 %, with a maximum of 2.8 %. This is below the maximum directional variation in S-wave velocities of single ice crystals of 12 % (Lutz and others, 2020).

The shear-wave splitting measurements have an overall mean fast S-wave direction (φ) of 29.3°N ± 18° (see Figure 3b). The uncertainty in this result is defined as one standard deviation, likely representing an upper estimate of uncertainty in the result that could be caused by temporal variations in φ (see Figure S2). Individual receivers generally have mean φ that fall within a range of 22.4°N to 47.0°N (see Figure 1b), with the exception of station WS07, which has a mean φ of 9.1°N (see label 07, Figure 1b). Ice core studies (Lipenkov and others, 1989; Wang and others, 2002; Weikusat and others, 2017) and seismic anisotropy studies (Kufner and others, 2023; Smith and others, 2017) have found that regions of longitudinal extension, such as ice divides and ice streams, have a vertical girdle fabric. In such fabrics, φ is found to be perpendicular to the ice flow direction (Harland and others, 2013). Based on ice flow direction derived from InSAR (Rignot and others, 2017) and the source polarisation data in Figure 3a, one would expect φ

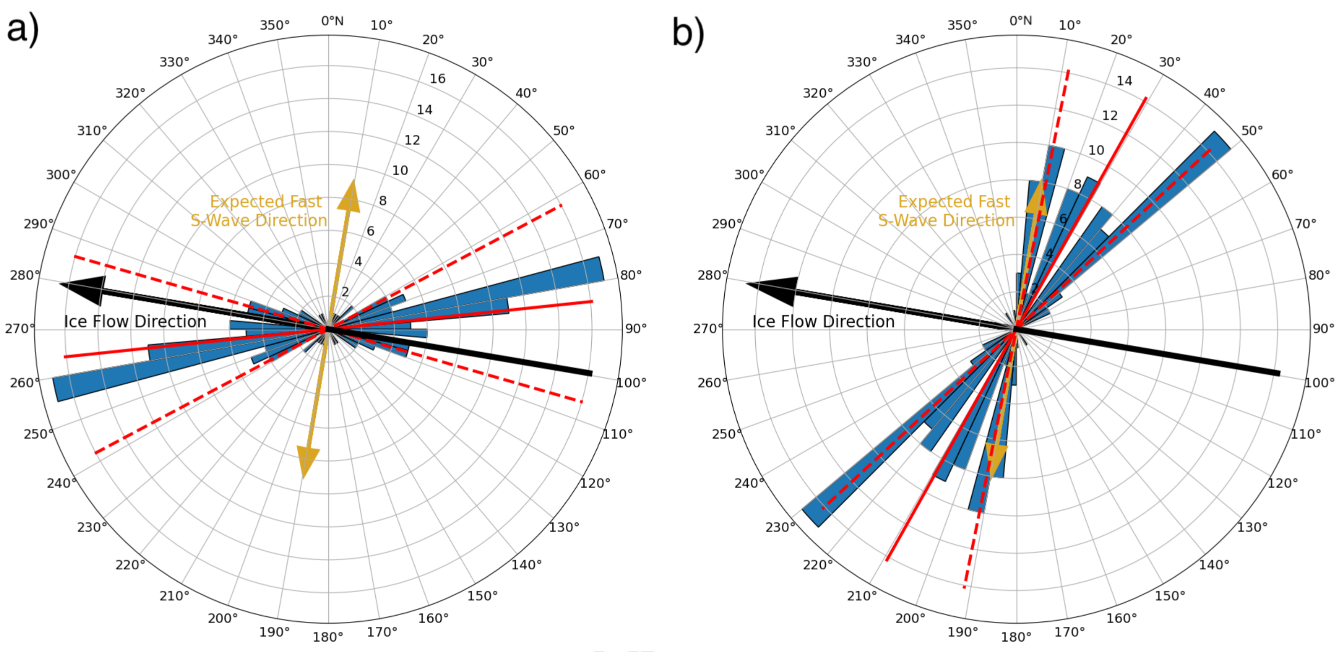

Fig. 3. Rose diagrams of (a) source polarisations and (b) fast S-wave directions for all the 80 SWS measurements. The solid and dotted red lines indicate the averages and uncertainties respectively. The gold arrows on both diagrams indicate the expected fast S-wave direction based on ice flow direction, which are shown as black arrows (see main text for further details). Method for estimating uncertainty is included in the supplementary information.

~10°N at the Whillans study site (golden arrow, Figure 3). However, the mean φ we observe of 29.3°N ± 18º is oblique to this expected fast S-wave direction of ~10°N, even after accounting for uncertainty. A t-test shows that the 95 % confidence interval of the fast S-wave directions lies in between 25.3°N and 33.3°N (assuming that the distribution of fast S-wave directions in the data is Gaussian), confirming our confidence in this obliquity.

DISCUSSION

Possible origins of an ice COF with an oblique fast S-wave direction

Our results suggest that the ice COF at Whillans Ice Stream (WIS) is oriented oblique, rather than perpendicular, to the ice flow direction. This obliqueness suggests one of two hypotheses: either that the local strain at our study site acts oblique to ice flow; or that the ice COF at WIS is the result of preservation of historic deformation upstream of the study site.

Regarding the first hypothesis, a possible reason for extension oblique to ice flow is the differential ice flux between the two tributaries of Whillans Ice Plain (WIP) across a suture zone. The study site is located downstream of the confluence between the upper WIS and Mercer Ice Stream (MIS), where the faster flow of WIS relative to MIS leads to shear strain across the suture zone, which can reorientate ice crystals (see Figure 4; Beem and others, 2014). However, Bindschadler and others (1987) argue that shear is minimal between WIS and MIS. Additionally, we postulate that this suture zone has a negligible effect on the ice COF at our study site because the significant mixing between the two ice streams in the suture zone would perturb the ice fabric on length scales of the order of hundreds of metres. This mixing would likely yield significant differences in the fast-polarisation S-wave azimuth (φ) between the different stations, yet the fast-polarisation S-wave azimuths remain constant within uncertainty across the network (see Figure 1b) and a dominant fast polarisation direction can be seen in Figure 3b. Nonetheless, even if our ice COF were to be affected by this shearing, the suture zone is located upstream of our study site (see high strain rates near the intersection of WIS and MIS in Figure 4) and therefore also supports the second hypothesis.

We instead favour the second hypothesis: that WIS has a "palaeo-COF" that preserves a record of WIS' upstream palaeo-deformation. Ice core studies and numerical simulations suggest that such preservation of a palaeo COF is possible (Faria, 2018; Llorens and others, 2022).This preservation can be partially explained by the concept of Microstructural Fading Memory, where polycrystalline ice can inherit microstructure imprints from sintering and deformation structures of former granular snow and porous firn (Faria, 2018). However, although this could explain some of the preservation, it likely does not explain the preservation of fabric in the entire column, especially near the ice-bed interface where air inclusions are likely minimal. We expect at least some of the anisotropic contribution to be from this deeper portion of the ice column near the ice-bed interface, as found in other studies (Kufner and others, 2023), so suggesting that other preservation mechanisms might also be at play. Most of the ice deformation at WIP occurs along the shear

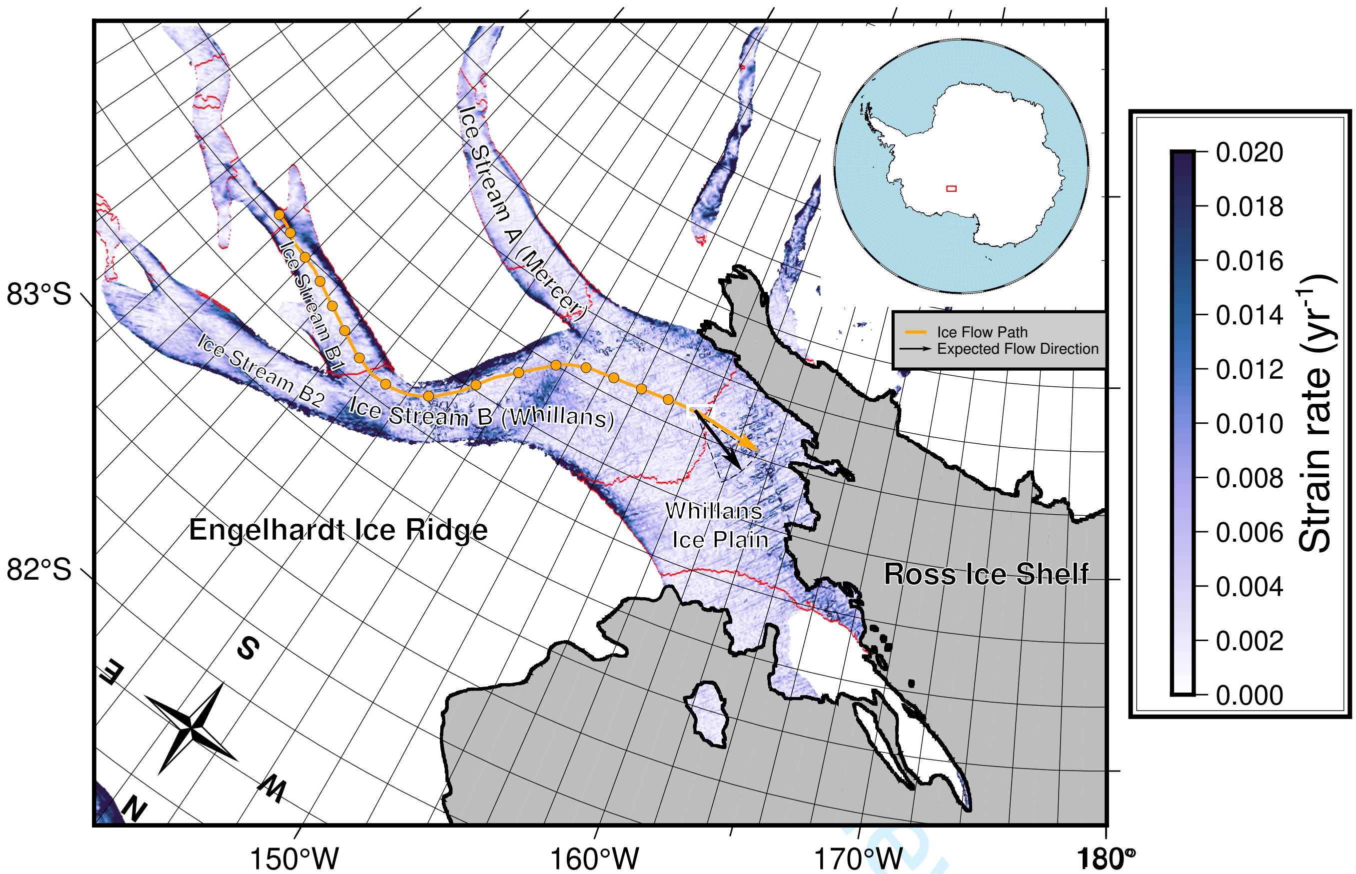

Fig. 4. A summary of the study findings. Regions with a flow direction between 281°N to 317°N, are shaded in red. The orange arrow shows the present-day flow direction. The black arrow indicates the flow direction inferred from the fast S-wave polarisation direction, and the dashed black sector outline shows the range of azimuths expressed by the red shaded regions. The background colour map is the strain rate calculated using Rignot and others (2017)'s velocity map (see supplementary information for calculation). Other features shown in this map are as in Figure 1a. The azimuth of the strain rate is shown in Figure S3.

margins (Truffer and Echelmeyer, 2003) and ice flow is mainly accommodated by basal slip, so internal deformation at Whillans is minimal. In such flow regimes, lattice rotation plays an important role relative to dynamic recrystallisation in ice fabric evolution (Azuma, 1994; Fan and others, 2021).

The c-axes of the ice crystals always rotate towards the principal direction of compression, which in ice streams is the azimuthal direction perpendicular to the flow direction (Smith and others, 2017; Thorsteinsson and others, 2003). The meandering nature of WIS alters the direction of compression, and therefore the ice COF—which in WIS evolves based on c-axis rotation—represents an integrated history of upstream strain induced by this changing stress. As such, it is difficult to pinpoint the origin of the fabric formation. However, for the ice COF to have developed the observed oblique φ, part of the integrated strain history must have originated from upstream areas in the ice stream where the flow direction was perpendicular to φ. Considering the present-day westward flow direction only and fast S-wave polarisation uncertainties of 18°, these regions have a flow direction approximately in the west-northwest direction of 281°N to 317°N (see shaded red regions in Figure 4). The nearest region with such a flow direction along the ice flow path is in the southern tributary of WIS, indicating that the ice COF could not have been purely derived from the integrated strain alone over the past 450 years. Consequently, this implies that the entire ice stream flow field of WIS changes on timescales shorter than ice COF re-equilibration. With this observation, we assumed constant flow directions with time because ice-flow chronological studies do not suggest major changes in flow direction at WIS over the past 500 years (Catania and others, 2012). Furthermore, the validity of this assumption does not affect our conclusion of a palaeo-COF at WIS because present-day ice velocity orientations are insufficient to explain the observed φ.

Larger strain rates can accelerate the rotation of lattices, which reduces the re-equilibration timescales of ice fabrics and causes the COF to inherit signatures of the local strain field. Therefore, the integrated strain history better preserves the fabric along flow where the strain is greater. From present-day velocities, the largest strain rates are located on the main trunk of WIS before it merges with the MIS (see Figure 4). However, these strain rates could have been different in the past because of the dynamic nature of ice streams. Some studies show that ice streams in the Ross Sea sector have variable mass fluxes over the past centuries, in particular the Kamb Ice Stream (Bougamont and others, 2015; Catania and others, 2012; Conway and others, 2002). Further studies of ice anisotropy, in combination with more detailed past ice conditions and flow calculations, would further evidence any dynamic changes in ice anisotropy along WIS.

Given that the expected φ based on current ice flow is only just outside the uncertainty of our results, we cannot ignore the possibility of an ice COF derived from the present-day study site. However, there is only a negligible part of the study area that has a flow direction between 281°N and 317°N, with the remainder of this region located downstream of the study site (see red shaded regions in Figure 4). Hence, it is unlikely that enough time elapses for the ice COF to re-equilibrate with the present-day flow direction. We therefore suggest that the ice fabric is most likely derived from upstream palaeo-deformation.

Comparison to other COF studies at WIS

Our results of an oblique fast S-wave direction (φ) differ from previous findings of an azimuth-independent fabric (Picotti and others, 2015) and a fabric with φ parallel to flow between 170 m and 400 m depth (Jordan and others, 2020). We attribute these differences to variations in sampling location and depth (see Figure 1a).

Jordan and others (2020) find two types of vertical girdle fabrics at different depths: a fabric with φ perpendicular to flow for ice up near the surface, and another fabric with φ parallel to flow up to 360 m deep. The former fabric agrees with our results, while the latter suggests a longitudinally compressive instead of longitudinally extensional stress regime, where compression and extension is defined as the principal compression axis being parallel and perpendicular to flow respectively. Because their study was conducted near the grounding line (see Figure 1a), we attribute the second girdle fabric (φ parallel to flow) to the influence of longitudinal compression due to stronger interactions between the ice and the bed topography near the grounding zone (Bindschadler and others, 1987; Picotti and others, 2015). If both fabrics are present in the ice column at our study site, then as we only invert for a single anisotropic layer, both fabric orientations would be represented as a single, composite result. If two perpendicular fabrics are present, then any shear-wave splitting measurements would be unable to discriminate between the layers, with the anisotropy amplitude (delay-time) being damped or amplified, but the overall orientation of anisotropy remaining constant. Other studies have suggested that the stress regime at WIP is longitudinally compressive (Bindschadler and others, 1987). However, this likely does not apply to our study site. Firstly, the strain rates at WIS vary massively as little as 20 kilometres (see Figure 9 of Bindschadler and others, 1987). Secondly, the ice flow path inferred from present-day velocities indicates that the ice at our study site has travelled along the outer part of the curve at WIP, where we expect the stress regime to be longitudinally extensional (see Figure 4). Because most of the vertical shear needed to accommodate the driving stress at WIS occurs within the basal sediment layer (MacAyeal, 1989), we expect the velocity orientation to be similar across all depths of the ice stream. Thirdly, the ice at our study site is located sufficiently far from the grounding line, such that it should not experience significant longitudinal compression from interactions between the ice and grounding line bed topography (Pattyn, 2000).

Picotti and others (2015) observe an azimuth-independent fabric across the entire ice column, and suggest that ice streams with low basal shear stress and highly-water-saturated sediments have COF profiles similar to ice divides due to the increasing influence of vertical compression relative to transverse compression. However, most of their study is based on surface wave data and traveltime inversions that could only image the fabric up to 200 m at WIS. Furthermore, their study site is located above Subglacial Lake Whillans, which is further inwards of the curve at WIP, where the stress regime is less longitudinally extensional (see Figure 1a). Additionally, their ice COF is likely to have undergone more equilibration caused by higher strain rates and lower flow velocities on the northern side of WIS (see Figure 4; Bindschadler and others, 1987). Given this variance in ice COF in WIS, future studies of ice deformation and anisotropy can furthermore reveal the spatial and temporal variability of ice COF at WIS.

Comparison to other ice streams

Shear-wave splitting studies from another Antarctic ice stream, Rutford Ice Stream (RIS), find that the COF at RIS is approximately perpendicular ($\sim 85^{\circ}$) to ice flow (Harland and others, 2013; Smith and others, 2017). Unlike the deviatoric nature of WIS stream flow, the flow direction at RIS is approximately linear over COF re-equilibration timescales. As such, it is not possible to discriminate to what extent the COF at RIS represents the current deformation or a preserved upstream deformation state. Kufner and others (2023) suggest that the RIS COF signal is dominated by the latter.

The strength of anisotropy at RIS is 3-5 %, while that at WIS is 1.5 %. This difference can be attributed to the driving stress, with the driving stress at RIS (40 kPa; Doake and others, 2001) at least twice that at WIS (<20 kPa; Bentley, 1987). The two ice streams have similar flowing speeds, with RIS moving at an average velocity of 377 ma^{-1} and WIS flowing at 370 ma^{-1} (Morlighem, 2022; Smith and others, 2017). Hence, the difference in driving stress is accommodated by the difference in basal friction. This can be explained by the relatively larger normal vertical stress at RIS of 10 – 500 kPa, compared to that at WIS of 20 – 30 kPa (Hudson and others, 2023b; Lipovsky and Dunham, 2016). The lower basal friction at WIS is a consequence of the weak till layer at WIS, such that the vertical shear strain rates required to support the driving stress are mostly confined within the basal till (Blankenship and others, 1986; MacAyeal, 1989).

This results in less internal deformation of the ice column, leading to lower strengths of anisotropy at WIS.

A recent seismic anisotropy study at RIS by Kufner and others (2023) suggested that multi-layer anisotropy can be present in ice streams, where the deepest third of the ice stream is thought to comprise an azimuthally isotropic cluster fabric caused by basal shearing (Azuma, 1994). However, the apparent absence of multiple fast S-wave phase arrivals in our data suggests that the effects of any multi-layer anisotropy at WIS are negligible, to which here we define multi-layer anisotropy as a type of depth-dependent anisotropy with sharper changes in anisotropic signatures with depth. Indeed we did not observe sufficient hints of multi-layer splitting to invert for multiple layers, even though such an inversion is possible at ice streams (Hudson and others, 2023a). Inverting for a multi-layer anisotropic model at WIS would introduce additional parameters on layer thicknesses and fast polarisation directions, which could result in overfitting of the data, compared to a single depth-integrated anisotropy model.

Because most of the vertical shear at WIS is accommodated within the basal sediment layer (MacAyeal, 1989), we would expect the surface velocity direction to represent the orientation of maximum strain with depth, except perhaps for a thin (1 to 10s metres) basal shear layer near the ice-bed interface, which could vary somewhat in orientation over short length scales (10s to 100s metres) due to local bed topography variations. The depth of ice affected by shearing will either be too thin to be observed in seismic lengthscales or too weak to affect the overall anisotropic signature of the ice stream (Bindschadler and others, 1987; Blankenship and others, 1986). Additionally, even if the shear zone were to exhibit strong anisotropy, the cluster fabric that would likely result is azimuthally isotropic and therefore has little effect on our results of a preferred c-axis azimuth. In summary, we therefore would expect the dominant anisotropy to be oriented relative to surface ice flow velocity.

Implications of an oblique ice fabric on ice flow

Ice with a COF with the c-axis of a girdle fabric oriented perpendicular to flow can flow up to ten times faster than isotropic ice, because the viscosity of ice is sixty times lower parallel to the a-axis (the plane of weakest viscosity in the anisotropic crystal structure) than the c-axis (Budd and Jacka, 1989; Duval and others, 1983; Pimienta and others, 1987). However, our results at WIS show a c-axis orientation that is not perpendicular, but oblique to ice flow, or equivalently a misalignment of the a-axis with the flow direction. Because of the lower viscosity along the a-axis, this misalignment implies that WIS is not deforming internally at its fastest possible rate. This misalignment likely also contributes to the observation of little internal deformation of Whillans Ice Plain (Truffer and Echelmeyer, 2003).

Our observations suggest that palaeo ice COF can somewhat control present-day ice flow. If the shape of an ice stream deviates on length scales less than the distance ice travels within the COF re-equilibration time, then the COF may not be aligned with ice flow, limiting the rate of deformation of the ice column with respect to ice flow direction. If an ice stream flows linearly for a duration greater than the re-equilibration time, then the COF should re-equilibrate with the bulk stress, such that the a-axis direction will rotate parallel to the ice flow direction and increase the rate of deformation downstream. The degree of re-equilibration of an ice COF with the surrounding stresses is not only dependent on ice stream shape, but also on flow speed. Slower-flowing ice will have more time to re-equilibrate with the surrounding stress-field. The long-term slowdown at WIS can therefore provide more time for its ice COF re-equilibration, which in turn reduces the misalignment of the a-axis with flow direction and allows for faster flow. This counteraction to the slowdown has consequences on future predictions of ice flow at WIS.

Most icesheet-scale ice dynamics models assume either that ice is isotropic, or parameterise anisotropy effects via an enhancement factor to account for ice weakening due to COF orientation relative to ice flow. However, recent studies such as Smith and others (2017) and Kufner and others (2023), suggest that enhancement factors should no longer be used to parameterise ice viscosity in fast deforming regions such as ice streams. Our findings at WIS further support the importance of characterising directionally-dependent ice viscosity in ice flow models, and emphasise that understanding ice COF in both space and time is important for producing more realistic deformation in ice dynamics models.

CONCLUSION

This study provides shear-wave splitting (SWS) observations from basal icequakes at Whillans Ice Stream (WIS). From these observations, we infer the ice crystal orientation fabric (COF) anisotropy over the entire ice column. The observations provide insight into past and present deformation at WIS. The results from 80 discrete icequakes SWS observations show that WIS has an average fast S-wave direction (φ) of 29.3°, which is oblique to the expected direction of $\sim$10° based on ice flow direction at the study site of around 280°. We suggest that the ice COF records an integrated strain history along its flow path for at least the past 450 years to have preserved deformation in the direction of φ. The non-perpendicularity of φ to ice flow implies that the shape of an ice stream can affect its flow, such that spatially deviatoric ice streams including WIS are not flowing at their fastest potential. Given the long-term slowdown of WIS, the a-axis will have more time to re-equilibrate with the surrounding stress-field, which can counteract the long-term slowdown. Our results have implications for ice sheet models, suggesting that historic ice flow can preserve ice fabric and hence directionally-dependent ice viscosity that might play an important role in such models.

SUPPLEMENTARY MATERIAL

The supplementary material for this article can be found in suppl_mat_WIS_anisotropy.pdf, as attached with the submission of this manuscript.

ACKNOWLEDGEMENTS

We thank Alex Brisbourne for his comments, which have improved the manuscript.

REFERENCES

Azuma N (1994) A flow law for anisotropic ice and its application to ice sheets. *Earth and Planetary Science Letters*, **128**(3-4), 601–614, ISSN 0012821X (doi: 10.1016/0012-821X(94)90173-2)

Barcheck CG, Tulaczyk S, Schwartz SY, Walter JI and Winberry JP (2018) Implications of basal micro-earthquakes and tremor for ice stream mechanics: Stick-slip basal sliding and till erosion. *Earth and Planetary Science Letters*, **486**, 54–60, ISSN 0012821X (doi: 10.1016/j.epsl.2017.12.046)

Barcheck CG, Schwartz SY and Tulaczyk S (2020) Icequake streaks linked to potential mega-scale glacial lineations beneath an Antarctic ice stream. *Geology*, **48**(2), 99–102, ISSN 0091-7613, 1943-2682 (doi: 10.1130/G46626.1)

Barcheck G, Brodsky EE, Fulton PM, King MA, Siegfried MR and Tulaczyk S (2021) Migratory earthquake precursors are dominant on an ice stream fault. *Sci. Adv.*, **7**(6), eabd0105, ISSN 2375-2548 (doi: 10.1126/sciadv.abd0105)

Beem LH, Tulaczyk SM, King MA, Bougamont M, Fricker HA and Christoffersen P (2014) Variable deceleration of Whillans Ice Stream, West Antarctica. *J. Geophys. Res. Earth Surf.*, **119**(2), 212–224, ISSN 21699003 (doi: 10.1002/2013JF002958)

Bentley CR (1987) Antarctic ice streams: A review. *J. Geophys. Res.*, **92**(B9), 8843, ISSN 0148-0227 (doi: 10.1029/JB092iB09p08843)

Bindschadler RA, Stephenson SN, MacAyeal DR and Shabtaie S (1987) Ice dynamics at the mouth of ice stream B, Antarctica. *J. Geophys. Res.*, **92**(B9), 8885, ISSN 0148-0227 (doi: 10.1029/JB092iB09p08885)

Bindschadler RA, King MA, Alley RB, Anandakrishnan S and Padman L (2003) Tidally controlled stick-slip discharge of a West Antarctic ice. *Science*, **301**(5636), 1087–1089

Blankenship DD, Bentley CR, Rooney ST and Alley RB (1986) Seismic measurements reveal a saturated porous layer beneath an active Antarctic ice stream. *Nature*, **322**(6074), 54–57, ISSN 0028-0836, 1476-4687 (doi: 10.1038/322054a0)

Bougamont M, Christoffersen P, Price SF, Fricker HA, Tulaczyk S and Carter SP (2015) Reactivation of Kamb Ice Stream tributaries triggers century-scale reorganization of Siple Coast ice flow in West Antarctica. *Geophysical Research Letters*, **42**(20), 8471–8480, ISSN 0094-8276, 1944-8007 (doi: 10.1002/2015GL065782)

Budd W and Jacka T (1989) A review of ice rheology for ice sheet modelling. *Cold Regions Science and Technology*, **16**(2), 107–144, ISSN 0165232X (doi: 10.1016/0165-232X(89)90014-1)

Catania G, Hulbe C, Conway H, Scambos T and Raymond C (2012) Variability in the mass flux of the Ross ice streams, West Antarctica, over the last millennium. *J. Glaciol.*, **58**(210), 741–752, ISSN 0022-1430, 1727-5652 (doi: 10.3189/2012JoG11J219)

Conway H, Catania G, Raymond CF, Gades AM, Scambos TA and Engelhardt H (2002) Switch of flow direction in an Antarctic ice stream. *Nature*, **419**(6906), 465–467, ISSN 0028-0836, 1476-4687 (doi: 10.1038/nature01081)

Doake CSM, Corr HFJ, Jenkins A, Makinson K, Nicholls KW, Nath C, Smith AM and Vaughan DG (2001) Rutford Ice Stream, Antarctica. In *The West Antarctic Ice Sheet: Behavior and Environment*, 221–235, American Geophysical Union (AGU), ISBN 978-1-118-66832-0 (doi: https://doi.org/10.1029/AR077p0221)

Duval P, Ashby MF and Anderman I (1983) Rate-controlling processes in the creep of polycrystalline ice. *J. Phys. Chem.*, **87**(21), 4066–4074, ISSN 0022-3654, 1541-5740 (doi: 10.1021/j100244a014)

Ester M, Kriegel HP, Sander J and Xu X (1996) A density-based algorithm for discovering clusters in large spatial databases with noise. In *Proceedings of the Second International Conference on Knowledge Discovery and Data Mining*, KDD'96, 226–231, AAAI Press, place: Portland, Oregon

Fan S, Cross AJ, Prior DJ, Goldsby DL, Hager TF, Negrini M and Qi C (2021) Crystallographic Preferred Orientation (CPO) Development Governs Strain Weakening in Ice: Insights From High-Temperature Deformation Experiments. *JGR Solid Earth*, **126**(12), e2021JB023173, ISSN 2169-9313, 2169-9356 (doi: 10.1029/2021JB023173)

Faria SH (2018) Slip-band distributions and microstructural fading memory beneath the firn–ice transition of polar ice sheets. *Mechanics Research Communications*, **94**, 95–101, ISSN 00936413 (doi: 10.1016/j.mechrescom.2018.09.009)

Fricker HA and Scambos T (2009) Connected subglacial lake activity on lower Mercer and Whillans Ice Streams, West Antarctica, 2003–2008. *J. Glaciol.*, **55**(190), 303–315, ISSN 0022-1430, 1727-5652 (doi: 10.3189/002214309788608813)

Harland S, Kendall JM, Stuart G, Lloyd G, Baird A, Smith A, Pritchard H and Brisbourne A (2013) Deformation in Rutford Ice Stream, West Antarctica: measuring shear-wave anisotropy from icequakes. *Ann. Glaciol.*, **54**(64), 105–114, ISSN 0260-3055, 1727-5644 (doi: 10.3189/2013AoG64A033)

Hudson TS, Brisbourne AM, Walter F, Gräff D, White RS and Smith AM (2020) Icequake Source Mechanisms for Studying Glacial Sliding. *JGR Earth Surface*, **125**(11), e2020JF005627, ISSN 2169-9003, 2169-9011 (doi: 10.1029/2020JF005627)

Hudson TS, Asplet J and Walker AM (2023a) Automated shear-wave splitting analysis for single- and multi- layer anisotropic media. *Seismica*, **2**(2), ISSN 2816-9387 (doi: 10.26443/seismica.v2i2.1031)

Hudson TS, Kufner SK, Brisbourne AM, Kendall JM, Smith AM, Alley RB, Arthern RJ and Murray T (2023b) Highly variable friction and slip observed at Antarctic ice stream bed. *Nat. Geosci.*, **16**(7), 612–618, ISSN 1752-0894, 1752-0908 (doi: 10.1038/s41561-023-01204-4)

Jordan TM, Schroeder DM, Elsworth CW and Siegfried MR (2020) Estimation of ice fabric within Whillans Ice Stream using polarimetric phase-sensitive radar sounding. *Ann. Glaciol.*, **61**(81), 74–83, ISSN 0260-3055, 1727-5644 (doi: 10.1017/aog.2020.6)

Kufner S, Wookey J, Brisbourne AM, Martín C, Hudson TS, Kendall JM and Smith AM (2023) Strongly Depth-Dependent Ice Fabric in a Fast-Flowing Antarctic Ice Stream Revealed With Icequake Observations. *JGR Earth Surface*, **128**(3), e2022JF006853, ISSN 2169-9003, 2169-9011 (doi: 10.1029/2022JF006853)

Lipenkov V, Barkov N, Duval P and Pimienta P (1989) Crystalline Texture of the 2083 m Ice Core at Vostok Station, Antarctica. *J. Glaciol.*, **35**(121), 392–398, ISSN 0022-1430, 1727-5652 (doi: 10.3189/S0022143000009321)

Lipovsky BP and Dunham EM (2016) Tremor during ice-stream stick slip. *The Cryosphere*, **10**(1), 385–399, ISSN 1994-0424 (doi: 10.5194/tc-10-385-2016)

Llorens MG, Griera A, Bons PD, Weikusat I, Prior DJ, Gomez-Rivas E, De Riese T, Jimenez-Munt I, García-Castellanos D and Lebensohn RA (2022) Can changes in deformation regimes be inferred from crystallographic preferred orientations in polar ice? *The Cryosphere*, **16**(5), 2009–2024, ISSN 1994-0424 (doi: 10.5194/tc-16-2009-2022)

Lomax A, Virieux J, Volant P and Berge-Thierry C (2000) Probabilistic Earthquake Location in 3D and Layered Models. In CH Thurber and N Rabinowitz (eds.), *Advances in Seismic Event Location*, 101–134, Springer Netherlands, Dordrecht, ISBN 978-94-015-9536-0 (doi: 10.1007/978-94-015-9536-0_5)

Lutz F, Eccles J, Prior DJ, Craw L, Fan S, Hulbe C, Forbes M, Still H, Pyne A and Mandeno D (2020) Constraining Ice Shelf Anisotropy Using Shear Wave Splitting Measurements from Active-Source Borehole Seismics. *JGR Earth Surface*, **125**(9), e2020JF005707, ISSN 2169-9003, 2169-9011 (doi: 10.1029/2020JF005707)

MacAyeal DR (1989) Large-scale ice flow over a viscous basal sediment: Theory and application to ice stream B, Antarctica. *J. Geophys. Res.*, **94**(B4), 4071–4087, ISSN 0148-0227 (doi: 10.1029/JB094iB04p04071)

Menke W and Levin V (2003) The cross-convolution method for interpreting *SKS* splitting observations, with application to one and two-layer anisotropic earth models. *Geophysical Journal International*, **154**(2), 379–392, ISSN 0956540X, 1365246X (doi: 10.1046/j.1365-246X.2003.01937.x)

Morgan V, Jacka T, Akerman G and Clarke A (1982) Outlet Glacier and Mass-Budget Studies in Enderby, Kemp, and Mac. Robertson Lands, Antarctica. *Ann. Glaciol.*, **3**, 204–210, ISSN 0260-3055, 1727-5644 (doi: 10.3189/S0260305500002780)

Morlighem M (2022) MEaSUREs BedMachine Antarctica, Version 3 (doi: 10.5067/FPSU0V1MWUB6)

Pattyn F (2000) Ice-sheet modelling at different spatial resolutions: focus on the grounding zone. *Ann. Glaciol.*, **31**, 211–216, ISSN 0260-3055, 1727-5644 (doi: 10.3189/172756400781820435)

Picotti S, Vuan A, Carcione JM, Horgan HJ and Anandakrishnan S (2015) Anisotropy and crystalline fabric of Whillans Ice Stream (West Antarctica) inferred from multicomponent seismic data. *JGR Solid Earth*, **120**(6), 4237–4262, ISSN 2169-9313, 2169-9356 (doi: 10.1002/2014JB011591)

Pimienta P, Duval P and Lipenkov VY (1987) Mechanical behavior of anisotropic polar ice. In *Proceedings of the Vancouver Symposium*, volume 170, 57–66, International Association of Hydrological Sciences

Pratt MJ, Winberry JP, Wiens DA, Anandakrishnan S and Alley RB (2014) Seismic and geodetic evidence for grounding-line control of Whillans Ice Stream stick-slip events: Whillans Ice Stream Stick-Slip Events. *J. Geophys. Res. Earth Surf.*, **119**(2), 333–348, ISSN 21699003 (doi: 10.1002/2013JF002842)

Rignot E, Mouginot J, Morlighem M and Scheuchl B (2017) MEaSUREs InSAR-Based Antarctica Ice Velocity Map, Version 2 (doi: 10.5067/D7GK8F5J8M8R)

Schwartz SY (2012) Whillians Ice Stream Subglacial Access Research Drilling (doi: 10.7914/SN/YD_2012)

Siegfried MR, Fricker HA, Carter SP and Tulaczyk S (2016) Episodic ice velocity fluctuations triggered by a subglacial flood in West Antarctica. *Geophysical Research Letters*, **43**(6), 2640–2648, ISSN 0094-8276, 1944-8007 (doi: 10.1002/2016GL067758)

Smith EC, Baird AF, Kendall JM, Martín C, White RS, Brisbourne AM and Smith AM (2017) Ice fabric in an Antarctic ice stream interpreted from seismic anisotropy. *Geophysical Research Letters*, **44**(8), 3710–3718, ISSN 0094-8276, 1944-8007 (doi: 10.1002/2016GL072093)

Teanby NA, Kenda NA, Kendall JM, Martin C, White RS, Brisbourne AM and Smith AM (2004) Automation of Shear-Wave Splitting Measurements using Cluster Analysis. *Bulletin of the Seismological Society of America*, **94**(2), 453–463, ISSN 0037-1106 (doi: 10.1785/0120030123)

Thorsteinsson T, Waddington ED and Fletcher RC (2003) Spatial and temporal scales of anisotropic effects in ice-sheet flow. *Ann. Glaciol.*, **37**, 40–48, ISSN 0260-3055, 1727-5644 (doi: 10.3189/172756403781815429)

Truffer M and Echelmeyer KA (2003) Of isbræ and ice streams. *Ann. Glaciol.*, **36**, 66–72, ISSN 0260-3055, 1727-5644 (doi: 10.3189/172756403781816347)

Walsh E, Arnold R and Savage MK (2013) Silver and Chan revisited: SILVER AND CHAN REVISITED. *J. Geophys. Res. Solid Earth*, **118**(10), 5500–5515, ISSN 21699313 (doi: 10.1002/jgrb.50386)

Walter JI, Brodsky EE, Tulaczyk S, Schwartz SY and Pettersson R (2011) Transient slip events from near-field seismic and geodetic data on a glacier fault, Whillans Ice Plain, West Antarctica: RUPTURE SPEEDS ON WHILLANS ICE PLAIN. *J. Geophys. Res.*, **116**(F1), n/a–n/a, ISSN 01480227 (doi: 10.1029/2010JF001754)

Walter JI, Svetlizky I, Fineberg J, Brodsky EE, Tulaczyk S, Grace Barcheck C and Carter SP (2015) Rupture speed dependence on initial stress profiles: Insights from glacier and laboratory stick-slip. *Earth and Planetary Science Letters*, **411**, 112–120, ISSN 0012821X (doi: 10.1016/j.epsl.2014.11.025)

Wang Y, Thorsteinsson T, Kipfstuhl J, Miller H, Dahl-Jensen D and Shoji H (2002) A vertical girdle fabric in the NorthGRIP deep ice core, North Greenland. *Ann. Glaciol.*, **35**, 515–520, ISSN 0260-3055, 1727-5644 (doi: 10.3189/172756402781817301)

Weikusat I, Jansen D, Binder T, Eichler J, Faria SH, Wilhelms F, Kipfstuhl S, Sheldon S, Miller H, Dahl-Jensen D and Kleiner T (2017) Physical analysis of an Antarctic ice core—towards an integration of micro- and macrodynamics of polar ice. *Phil. Trans. R. Soc. A.*, **375**(2086), 20150347, ISSN 1364-503X, 1471-2962 (doi: 10.1098/rsta.2015.0347)

Winberry JP, Anandakrishnan S, Alley RB, Bindschadler RA and King MA (2009) Basal mechanics of ice streams: Insights from the stick-slip motion of Whillans Ice Stream, West Antarctica. *J. Geophys. Res.*, **114**(F1), F01016, ISSN 0148-0227 (doi: 10.1029/2008JF001035)

Winberry JP, Anandakrishnan S, Wiens DA, Alley RB and Christianson K (2011) Dynamics of stick–slip motion, Whillans Ice Stream, Antarctica. *Earth and Planetary Science Letters*, **305**(3-4), 283–289, ISSN 0012821X (doi: 10.1016/j.epsl.2011.02.052)

Winberry JP, Anandakrishnan S, Wiens DA and Alley RB (2013) Nucleation and seismic tremor associated with the glacial earthquakes of Whillans Ice Stream, Antarctica. *Geophysical Research Letters*, **40**(2), 312–315, ISSN 0094-8276, 1944-8007 (doi: 10.1002/grl.50130)

Winberry JP, Anandakrishnan S, Alley RB, Wiens DA and Pratt MJ (2014) Tidal pacing, skipped slips and the slowdown of Whillans Ice Stream, Antarctica. *J. Glaciol.*, **60**(222), 795–807, ISSN 0022-1430, 1727-5652 (doi: 10.3189/2014JoG14J038)

Wuestefeld A, Al-Harrasi O, Verdon JP, Wookey J and Kendall JM (2010) A strategy for automated analysis of passive microseismic data to image seismic anisotropy and fracture characteristics: A strategy for automated analysis of passive microseismic data. *Geophysical Prospecting*, **58**(5), 755–773, ISSN 00168025 (doi: 10.1111/j.1365-2478.2010.00891.x)